

DYNAMIC VERSUS CONVENTIONAL LAYER SORTING FOR NULLING-AND-CANCELLING BASED MIMO DETECTION*

Dominik Seethaler[†], Harold Artés[‡], and Franz Hlawatsch[†]

[†]Institute of Communications and Radio-Frequency Engineering, Vienna University of Technology
 Gusshausstrasse 25/389, A-1040 Vienna, Austria
 Phone: +43 1 58801 38958, Fax: +43 1 58801 38999, E-mail: dominik.seethaler@tuwien.ac.at

[‡]Information Systems Laboratory, Stanford University
 Packard 234, 350 Serra Mall, Stanford, CA 94305-9510, USA

ABSTRACT

We analyze the error performance and computational complexity of the recently proposed *dynamic nulling-and-cancelling (DNC)* method for efficient near-ML MIMO detection. DNC performs a “dynamic” layer sorting (LS) that exploits the information provided by the current received vector, in contrast to conventional LS that is based merely on average reliability measures. Here, we derive an expression for the symbol error probability of the first layer-decoding step of DNC under some simplifying assumptions. This analysis as well as experimental results show the general superiority of dynamic LS and reveal the conditions under which this superiority will be most significant. We furthermore study how the two LS strategies impact the computational complexity of the (D)NC method. Specifically, we show that for practical system sizes the complexity of DNC is only about twice that of NC and only a fraction of that of the sphere-decoding algorithm for ML detection.

1. INTRODUCTION

Dynamic nulling-and-cancelling (DNC) has recently been proposed as an improved nulling-and-cancelling (NC) technique for MIMO detection [1]. In contrast to conventional NC [2, 3], which uses layer sorting (LS) according to the layerwise post-equalization signal-to-noise ratios, DNC uses a “dynamic” LS that exploits the information provided by the current received vector.

Here, we investigate and compare the performance of conventional and dynamic LS both analytically and experimentally. In [1], we demonstrated that for spatial multiplexing systems, DNC significantly outperforms NC and can achieve near-ML performance. Complementing these previous results, we now study the conditions under which the performance gains of dynamic LS can be expected to be significant or only small. We show that the performance gains will be strongest when conventional LS fails to exploit all degrees of freedom available for LS. On the other hand, we also show that dynamic LS will almost reduce to conventional LS when conventional LS has a strong preference for a specific layer.

After describing the system model and briefly reviewing the principle of NC in this section, we summarize conventional and dynamic LS in Section 2. In Section 3, we study the error performance of conventional and dynamic LS. For two statistically independent Gaussian layers, we derive an expression for the symbol error probability of the first layer-decoding step of DNC and discuss its consequences. Simulation results show that these analytical results extend to other, more general situations. In Section 4, we assess and compare the computational complexity of DNC and NC through estimates of complexity orders and simulation results.

1.1 System Model

We consider a linear MIMO model that describes several different space-time transmission schemes, including spatial multiplex-

ing systems such as V-BLAST [2] and systems using linear dispersion codes [4]. The transmitted data vector $\mathbf{d} \triangleq (d_1 \cdots d_M)^T$ of size M and the received vector $\mathbf{r} \triangleq (r_1 \cdots r_N)^T$ of size $N \geq M$ are related according to

$$\mathbf{r} = \mathbf{H}\mathbf{d} + \mathbf{w}.$$

Here, \mathbf{H} denotes the system matrix of size $N \times M$ and $\mathbf{w} \triangleq (w_1 \cdots w_N)^T$ is a noise vector. The data vector components d_k ($k \in \{1, \dots, M\}$ indexes the *layer*) are drawn from a complex symbol alphabet \mathcal{A} and assumed zero-mean and independent with unit variance. The noise components w_k are assumed independent and circularly symmetric complex Gaussian with variance σ_w^2 . The system matrix \mathbf{H} is supposed to be known at the receiver.

1.2 Review of Nulling-and-Cancelling

NC is a decision-feedback method that detects the layers one after another [2, 3]. At the first decoding step, the transmitted data vector \mathbf{d} is estimated as $\mathbf{y} = \mathbf{G}\mathbf{r}$, with the zero-forcing (ZF) equalizer $\mathbf{G}_{\text{ZF}} = (\mathbf{H}^H \mathbf{H})^{-1} \mathbf{H}^H$ or the minimum mean-square error (MMSE) equalizer $\mathbf{G}_{\text{MMSE}} = (\mathbf{H}^H \mathbf{H} + \sigma_w^2 \mathbf{I})^{-1} \mathbf{H}^H$ [5]. Then, the symbol of a certain layer $k_1 \in \{1, \dots, M\}$ is detected by quantizing $y_{k_1} = (\mathbf{G}\mathbf{r})_{k_1}$ according to the symbol alphabet \mathcal{A} , i.e.,

$$\hat{d}_{k_1} = Q\{y_{k_1}\} \triangleq \arg \min_{a \in \mathcal{A}} |y_{k_1} - a|^2. \quad (1)$$

Next, the interference caused by \hat{d}_{k_1} is subtracted from \mathbf{r} :

$$\mathbf{r}^{(2)} = \mathbf{r} - (\mathbf{H})_{k_1} \hat{d}_{k_1},$$

where $(\mathbf{H})_{k_1}$ denotes the k_1 th column of \mathbf{H} . If $\hat{d}_{k_1} = d_{k_1}$ (correct decision), we obtain the reduced system model

$$\mathbf{r}^{(2)} = \mathbf{H}^{(2)} \mathbf{d}^{(2)} + \mathbf{w}. \quad (2)$$

Here, $\mathbf{H}^{(2)}$ is \mathbf{H} without the k_1 th column and $\mathbf{d}^{(2)}$ is \mathbf{d} without the k_1 th component. At the second decoding step, the remaining layers are re-indexed as $\{1, \dots, M\} \setminus \{k_1\} \rightarrow \{1, \dots, M-1\}$, and a layer $k_2 \in \{1, \dots, M-1\}$ is detected using the reduced system model (2). This gives $\hat{d}_{k_2}^{(2)} = Q\{(\mathbf{G}^{(2)} \mathbf{r}^{(2)})_{k_2}\}$, where $\mathbf{G}^{(2)}$ is the ZF or MMSE equalizer for $\mathbf{H}^{(2)}$. Subsequently, the interference caused by $\hat{d}_{k_2}^{(2)}$ is subtracted from $\mathbf{r}^{(2)}$. This detection-subtraction procedure is repeated until all M layers are detected.

This basic principle of NC holds also for DNC. However, DNC uses—apart from the different LS technique—MMSE equalization with a different (“unbiased”) quantization of the MMSE equalizer outputs $y_{\text{MMSE},k}$. The standard quantization (1) is replaced by [1]

$$\hat{d}_{k_1} = \arg \min_{a \in \mathcal{A}} \psi_{k_1}(a), \quad \text{with } \psi_{k_1}(a) \triangleq \left| \frac{y_{\text{MMSE},k_1}}{W_{k_1}} - a \right|, \quad (3)$$

*This work was supported by FWF grant P15156-N02.

where W_{k_1} is the k_1 th diagonal element of the matrix $(\mathbf{I} + \sigma_w^2(\mathbf{H}^H\mathbf{H})^{-1})^{-1}$. (Note that $0 < W_{k_1} \leq 1$.) This quantization is equivalent to (1) for constant-modulus symbol alphabets but yields slight performance improvements otherwise.

2. LAYER SORTING

The main difference between DNC and conventional MMSE-based NC is the LS technique employed. The performance of NC schemes depends crucially on the *order* of the layers k_1, \dots, k_M . LS is based on the general principle that more reliable layers should be detected first [2]. This reduces error propagation effects and supports the processing of unreliable layers by means of the additional degrees of diversity that become available in the reduced system models.

We now summarize conventional and dynamic LS for the *first* layer-decoding step, where we detect layer k_1 in favor of a symbol \hat{d}_{k_1} . The subsequent layer-decoding steps are analogous, however with a reduced number of active layers.

The reliability criterion used by *conventional* LS within MMSE-based NC is given by the layerwise MMSE post-equalization signal-to-noise ratios (PSNRs) [2, 3], which can be expressed as (e.g. [6])

$$\text{SNR}_k = \frac{1}{\sigma_w^2 [(\mathbf{H}^H\mathbf{H} + \sigma_w^2\mathbf{I})^{-1}]_{k,k}} - 1.$$

The layers are sorted according to maximum PSNR, i.e.,

$$k_1 = \arg \max_{k \in \{1, \dots, M\}} \text{SNR}_k. \quad (4)$$

NC with this LS rule outperforms NC without LS but still is far inferior to ML detection (see Section 3.2). It is important to note that SNR_k is just an *average* reliability measure that does not depend on the received vector \mathbf{r} .

The *dynamic* LS rule underlying the DNC scheme was derived in [1] by means of a Gaussian approximation for the post-equalization interference. It reads as

$$k_1 = \arg \max_{k \in \{1, \dots, M\}} \left\{ \text{SNR}_k \min_{a \in \mathcal{A}(\hat{d}_k)} \{ \psi_k^2(a) - \psi_k^2(\hat{d}_k) \} \right\}, \quad (5)$$

where $\mathcal{A}(\hat{d}_k) \triangleq \mathcal{A} \setminus \{\hat{d}_k\}$ is the set of all symbols $a \neq \hat{d}_k$ and \hat{d}_k and $\psi_k(\cdot)$ have been defined in (3). Comparing (5) with (4), we see that SNR_k is augmented by the *instantaneous reliability factor* (IRF) $\min_{a \in \mathcal{A}(\hat{d}_k)} \{ \psi_k^2(a) - \psi_k^2(\hat{d}_k) \} \geq 0$. The term ‘‘instantaneous’’ refers to the fact that the IRF depends on the received vector \mathbf{r} via $y_{\text{MMSE},k}$ in (3). Whereas SNR_k merely measures the average reliability of equalization, the IRF measures the instantaneous reliability of the subsequent detection (quantization) process.

3. ERROR PERFORMANCE

In this section, we study the error performance of the first layer-decoding step of conventional and dynamic LS both analytically and through simulation. The first layer-decoding step is important because it has a decisive impact on the overall error performance of NC schemes.

3.1 Error Probability of a Two-Layer BPSK System

For tractability, we assume the case of two layers and BPSK modulation, with the two components of \mathbf{y}_{MMSE} being statistically independent and Gaussian. (In Section 3.2, we will verify that the results obtained are consistent with the performance observed when these simplifying assumptions are not satisfied.) The system matrix \mathbf{H} is considered fixed.

For BPSK modulation, dynamic LS in (5) simplifies as

$$k_1 = \arg \max_{k \in \{1, \dots, M\}} \{ \text{SNR}_k \hat{d}_k z_k \}, \quad \text{with } z_k \triangleq \frac{\text{Re}\{y_{\text{MMSE},k}\}}{W_k},$$

where \hat{d}_k is the result of conventional MMSE detection, i.e., $\hat{d}_k = Q\{y_{\text{MMSE},k}\} = \text{sgn}(\text{Re}\{y_{\text{MMSE},k}\}) = \text{sgn}(z_k)$. Hence,

$$k_1 = \arg \max_{k \in \{1, \dots, M\}} \{ \text{SNR}_k |z_k| \}.$$

We have

$$z_k = d_k + n_k \quad (6)$$

with some n_k independent of d_k . By the Gaussian approximation for the post-equalization interference, n_k is zero-mean Gaussian with variance $\sigma_{n_k}^2 = 1/(2 \text{SNR}_k)$. The error probability of MMSE detection for the k th layer is thus given by [7]

$$P[\hat{d}_k \neq d_k] = Q(\sqrt{2 \text{SNR}_k}), \quad (7)$$

where $Q(\cdot)$ denotes the Q-function. This result is valid for both NC and DNC. For conventional NC (i.e., LS according to maximum PSNR $\text{SNR}_{\text{max}} = \max_{k \in \{1, \dots, M\}} \text{SNR}_k$), the error probability of the first layer-decoding step follows as

$$P_{\text{conv}}[\mathcal{E}] = Q(\sqrt{2 \text{SNR}_{\text{max}}}).$$

For DNC, however, calculation of the error probability cannot be based on (7) because of the dynamic LS employed. It is shown in the Appendix that for two statistically independent active layers using BPSK symbols and under the Gaussian assumption, the error probability of the first layer-decoding step is given by

$$P_{\text{dyn}}[\mathcal{E}] = Q\left(\sqrt{2(\text{SNR}_1 + \text{SNR}_2)}\right). \quad (8)$$

Thus, whereas the error probability of conventional LS is determined by the *maximum* of the two PSNRs, the error probability of dynamic LS is determined by the *sum* of the two PSNRs. We can draw the following conclusions.

- Since $\text{SNR}_1 + \text{SNR}_2 \geq \max\{\text{SNR}_1, \text{SNR}_2\}$ and $Q(\cdot)$ is a decreasing function, the error probability of dynamic LS is upper bounded by the error probability of conventional LS, i.e.,

$$P_{\text{dyn}}[\mathcal{E}] \leq P_{\text{conv}}[\mathcal{E}].$$

- When one of the two PSNRs is very dominant, i.e., in the extreme case $\text{SNR}_1/\text{SNR}_2 \rightarrow \infty$ or $\text{SNR}_2/\text{SNR}_1 \rightarrow \infty$, the two error probabilities become equal, i.e., $P_{\text{dyn}}[\mathcal{E}] \rightarrow P_{\text{conv}}[\mathcal{E}]$. In fact, dynamic LS here chooses the layer with maximum PSNR and thus reduces to conventional LS.
- The performance gain of dynamic LS is most significant for equal PSNRs, i.e., $\text{SNR}_1 = \text{SNR}_2$. In this case, we obtain $P_{\text{conv}}[\mathcal{E}] = Q(\sqrt{2 \text{SNR}_1})$ and $P_{\text{dyn}}[\mathcal{E}] = Q(\sqrt{4 \text{SNR}_1})$. In fact, whereas conventional LS here fails (i.e., reduces to the case of no LS), dynamic LS achieves better performance because it exploits the information carried by the IRF.

We can conclude that the overall performance improvement due to dynamic LS strongly depends on the structure of the PSNRs associated with the realizations of \mathbf{H} . In Section 3.2, this will be verified experimentally for larger MIMO systems and a larger alphabet.

In [8], it has been shown that for an increasing size of the system matrix, *all* MMSE PSNRs associated with an iid system matrix converge to the *same* deterministic value. In the case of a spatial multiplexing system (where the system matrix equals the channel matrix), we can thus expect that the performance gain of DNC over

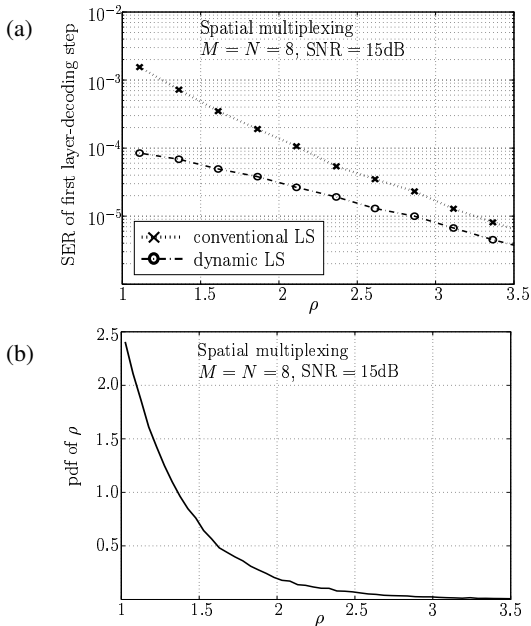


Figure 1: Simulation results demonstrating the error performance of the first layer-decoding step of DNC and conventional NC for a spatial multiplexing system with $M = N = 8$ and a 4-QAM symbol alphabet. (a) SER versus PSNR ratio ρ (see text) of the channel realization, (b) estimated pdf of ρ .

NC is stronger for a larger number of transmit and receive antennas (this has been verified experimentally in [1]). A strong average performance gain can also be expected if for each realization of the system matrix \mathbf{H} the PSNRs are grouped into subsets of equal PSNRs. Examples are the equivalent real-valued representation of spatial multiplexing systems using QAM signaling (verified experimentally in [1]) and systems using linear dispersion codes [4] (see Section 3.2).

3.2 Simulation Results

We will now assess the symbol error rate (SER) performance of DNC (dynamic LS) and conventional NC (conventional LS) through simulations. Note that we no longer use the simplifying assumptions made in Section 3.1. The MIMO channel was modeled iid Gaussian.

SPATIAL MULTIPLEXING SYSTEM. For a spatial multiplexing system, \mathbf{H} is the MIMO channel matrix and M and N are the numbers of transmit and receive antennas, respectively. Fig. 1(a) shows the simulated SER of the first layer-decoding step for a spatial multiplexing system of size $M = N = 8$ with 4-QAM symbol alphabet and a channel SNR of 15dB. The SER is plotted versus the ratio of the largest to second largest PSNR, which is denoted as ρ . The performance gain of dynamic LS over conventional LS is seen to be strongest when the two largest PSNRs are nearly equal, i.e., for $\rho \approx 1$; dynamic LS here achieves an SER reduction by a factor of about 20. However, the performance gain becomes quite small when one of the PSNRs is dominant (e.g., for $\rho = 3$ the SER is reduced just by a factor of about 1.5). This is an experimental verification of the theoretical results of Section 3.1.

Evidently, the average SER performance of the first layer-decoding step depends on the distribution of ρ . Fig. 1(b) shows an estimated probability density function (pdf) of ρ . It can be seen that for this system, small values of ρ are very likely. Thus we can expect that DNC achieves a significant reduction of the average SER of the first layer-decoding step, which yields a significant reduction of the overall SER. This has been verified experimentally in [1].

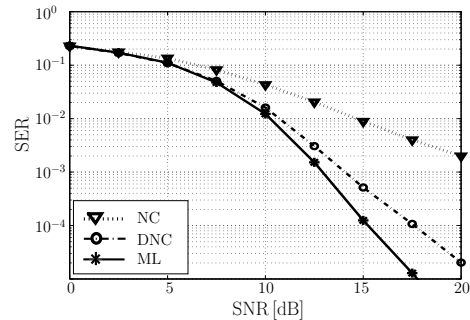


Figure 2: SER-versus-SNR performance of DNC, conventional NC, and optimum ML detection for a MIMO system using an LD code.

SYSTEM USING LINEAR DISPERSION CODE. Next, we consider a MIMO system where *all* PSNRs associated with the system matrix \mathbf{H} are exactly equal. This is the case for the linear dispersion (LD) code in [4, equation (31)]. We used 3 transmit antennas, 3 receive antennas, and a 4-QAM symbol alphabet. The size of \mathbf{H} was 18×18 . Fig. 2 shows the SER-versus-SNR performance (note that the overall SER is shown, not just the SER of the first layer-decoding step). We see that DNC substantially outperforms conventional NC and comes quite close to ML performance.

4. COMPUTATIONAL COMPLEXITY

The computational complexity of MMSE-based NC and DNC is dominated by the calculation of the equalizer matrices $\mathbf{G}_{\text{MMSE}}^{(l)}$, $l = 1, \dots, M$ (see Section 1.2). For NC, the LS just depends on the system matrix \mathbf{H} , and thus the equalizers $\mathbf{G}_{\text{MMSE}}^{(l)}$ are calculated only once for an entire block of vectors during which \mathbf{H} is approximately constant (hence, this contributes to the “preparation complexity” C_{prep}). For DNC, due to the dynamic LS employed, the reduced equalizers $\mathbf{G}_{\text{MMSE}}^{(l)}$, $l = 2, \dots, M$ have to be calculated anew for *each* received vector \mathbf{r} (hence, this contributes to the “vector complexity” C_{vector}). Thus, when \mathbf{H} is constant during several transmissions, the complexity of calculating the equalizers is higher for DNC than for NC.

Fortunately, for DNC C_{vector} can be significantly reduced by means of a recursive algorithm for calculating the equalizer matrices. While this algorithm was originally proposed for conventional NC [9], it yields larger benefits for DNC since for NC only C_{prep} is reduced. Using this recursive calculation for both NC and DNC, and assuming $N = M$ for simplicity, the preparation complexity (per block) C_{prep} is of order $\mathcal{O}(M^3)$ for both NC and DNC, and the vector complexity (per vector) C_{vector} is $\mathcal{O}(M^2)$ for NC and $\mathcal{O}(M^3)$ for DNC. However, we shall show next that for practical system sizes, C_{vector} for DNC is not much higher than for NC.

In Table 1, we present empirical complexity (kflo) estimates for NC, DNC, and ML detection in the case of spatial multiplexing systems with equal numbers of transmit and receive antennas $M = N \in \{4, 6, 8\}$ and a 4-QAM symbol alphabet¹. These kflo estimates were measured using MATLAB V5.3. Even though they are implementation-dependent, they may be more practically meaningful than the $\mathcal{O}(\cdot)$ complexity estimates presented above. We again distinguish between the preparation complexity C_{prep} and the vector complexity C_{vector} . The ML detector was implemented by means of the sphere-decoding (SD) algorithm [10]. The complexity of SD strongly depends on the SNR and the specific channel realization. Therefore, in addition to SD’s average C_{vector} , Table 1 shows SD’s maximum C_{vector} observed during 10000 simulation runs at an SNR of 10dB.

¹Note that for higher-order constellations the NC and the DNC complexity is just slightly increased.

System size $M=N$	Preparation complexity			Vector complexity			
	ML(SD)	DNC	NC	ML(SD) av. max.		DNC	NC
4	2.1	2.2	2.3	3.1	24.6	1.2	0.6
6	6.4	6.5	7.0	13.6	106.2	3.3	1.5
8	14.2	14.4	15.7	69.5	768	6.9	3.2

Table 1: Measured computational complexity (in *kflops*) of NC, DNC, and ML (sphere decoding) detection for spatial multiplexing systems with a 4-QAM symbol alphabet.

The following conclusions can be drawn from Table 1. For DNC, C_{vector} is about twice as large as for NC. C_{prep} is smaller for DNC than for NC, because with DNC a part of C_{prep} is transferred to C_{vector} . DNC's C_{vector} is just a fraction of both the average and maximum C_{vector} of SD (even though DNC can achieve near-ML performance). Note that in many applications C_{vector} will be the dominant complexity component.

5. CONCLUSIONS

The error probability analysis for dynamic layer sorting (LS) presented in this paper shows when and why dynamic nulling-and-cancelling (DNC) is able to outperform conventional nulling-and-cancelling (NC). The performance gain of dynamic LS is largest when the layerwise post-equalization signal-to-noise ratios (PSNRs) are all equal (in which case conventional LS fails), and smallest when one of the PSNRs is very dominant (in which case dynamic LS almost reduces to conventional LS). This behavior has been verified experimentally. Furthermore, for a MIMO system using a linear dispersion code, our simulation results showed that DNC significantly outperforms conventional NC and that it is able to come close to ML performance. This complements similar results for spatial multiplexing systems presented in [1].

Finally, an experimental complexity analysis demonstrated that for practical system sizes the computational complexity of DNC is only about twice that of NC and only a fraction of that of the sphere-decoding algorithm for ML detection.

APPENDIX: DERIVATION OF $P_{\text{dyn}}[\mathcal{E}]$ IN (8)

We derive the expression (8) for the error probability $P_{\text{dyn}}[\mathcal{E}]$ of the first layer-decoding step of DNC for the case of two active layers using BPSK modulation. Because of symmetry, $P_{\text{dyn}}[\mathcal{E}]$ is equal to the conditional error probability given any specific choice of transmitted symbols d_1 and d_2 , e.g., $d_1 = d_2 = 1$:

$$P_{\text{dyn}}[\mathcal{E}] = P_{\text{dyn}}[\mathcal{E} | d_1 = d_2 = 1].$$

We recall from Section 3.1 that the layer-sorting and symbol-detection rules are respectively given by

$$k_1 = \arg \max_{k \in \{1,2\}} \{\text{SNR}_k | z_k | \}, \quad \hat{d}_{k_1} = \text{sgn}(z_{k_1}).$$

Therefore, an error at the first layer-decoding step occurs either if DNC decodes in favor of layer 1 ($|z_1| > \frac{\text{SNR}_2}{\text{SNR}_1} |z_2|$) and makes a detection error ($\hat{d}_1 \neq 1$ or equivalently $z_1 < 0$), or if DNC decodes in favor of layer 2 ($|z_2| > \frac{\text{SNR}_1}{\text{SNR}_2} |z_1|$) and makes a detection error ($\hat{d}_2 \neq 1$ or equivalently $z_2 < 0$). Since these two events are mutually exclusive, we obtain

$$P_{\text{dyn}}[\mathcal{E}] = \mathbb{P} \left[-z_1 > \frac{\text{SNR}_2}{\text{SNR}_1} |z_2|, z_1 < 0 \mid d_1 = d_2 = 1 \right] \\ + \mathbb{P} \left[-z_2 > \frac{\text{SNR}_1}{\text{SNR}_2} |z_1|, z_2 < 0 \mid d_1 = d_2 = 1 \right].$$

It can be shown that this can be equivalently written as

$$P_{\text{dyn}}[\mathcal{E}] = \mathbb{P} \left[z_1 < -\frac{\text{SNR}_2}{\text{SNR}_1} z_2 \mid d_1 = d_2 = 1 \right].$$

Assuming that z_1 and z_2 (cf. (6)) are statistically independent and Gaussian, we obtain further

$$P_{\text{dyn}}[\mathcal{E}] = \frac{1}{2\pi \sigma_{n_1} \sigma_{n_2}} \int_{-\infty}^{\infty} \int_{-\infty}^{-\frac{\text{SNR}_2}{\text{SNR}_1} z_2} \exp \left(-\frac{1}{2} \left(\frac{z_1 - 1}{\sigma_{n_1}} \right)^2 \right) \\ \times \exp \left(-\frac{1}{2} \left(\frac{z_2 - 1}{\sigma_{n_2}} \right)^2 \right) dz_1 dz_2 \\ = \frac{1}{\sqrt{2\pi} \sigma_{n_2}} \int_{-\infty}^{\infty} \mathbb{Q} \left(\frac{\frac{\text{SNR}_2}{\text{SNR}_1} z_2 + 1}{\sigma_{n_1}} \right) \\ \times \exp \left(-\frac{1}{2} \left(\frac{z_2 - 1}{\sigma_{n_2}} \right)^2 \right) dz_2 \\ = \frac{1}{\sqrt{2\pi}} \int_{-\infty}^{\infty} \mathbb{Q} \left(\sqrt{\frac{\text{SNR}_2}{\text{SNR}_1}} x + \sqrt{\frac{2}{\text{SNR}_1}} (\text{SNR}_1 \right. \\ \left. + \text{SNR}_2) \right) e^{-x^2/2} dx,$$

where we used $\sigma_{n_k} = 1/\sqrt{2 \text{SNR}_k}$. Finally, by applying the identity (e.g. [11])

$$\frac{1}{\sqrt{2\pi}} \int_{-\infty}^{\infty} \mathbb{Q}(\lambda x + \mu) e^{-x^2/2} dx = \mathbb{Q} \left(\frac{\mu}{\sqrt{1 + \lambda^2}} \right),$$

we obtain $P_{\text{dyn}}[\mathcal{E}] = \mathbb{Q}(\sqrt{2(\text{SNR}_1 + \text{SNR}_2)})$, which is (8).

REFERENCES

- [1] D. Seethaler, H. Artés, and F. Hlawatsch, "Dynamic nulling-and-cancelling with near-ML performance," in *Proc. IEEE ICASSP 2004*, vol. IV, (Montreal, Canada), pp. 777–780, May 2004.
- [2] P. W. Wolniansky, G. J. Foschini, G. D. Golden, and R. A. Valenzuela, "V-BLAST: An architecture for realizing very high data rates over the rich-scattering wireless channel," in *Proc. URSI Int. Symp. on Signals, Systems and Electronics*, (Pisa, Italy), pp. 295–300, Sept. 1998.
- [3] B. Hassibi, "A fast square-root implementation for BLAST," in *Proc. 34th Asilomar Conf. Signals, Systems, Computers*, (Pacific Grove, CA), pp. 1255–1259, Nov./Dec. 2000.
- [4] B. Hassibi and B. Hochwald, "High-rate codes that are linear in space and time," *IEEE Trans. Inf. Theory*, vol. 48, no. 7, pp. 1804–1824, 2002.
- [5] S. M. Kay, *Fundamentals of Statistical Signal Processing: Estimation Theory*. Englewood Cliffs (NJ): Prentice Hall, 1993.
- [6] R. W. Heath, S. Sandhu, and A. J. Paulraj, "Antenna selection for spatial multiplexing systems with linear receivers," *IEEE Commun. Letters*, vol. 5, pp. 142–144, April 2001.
- [7] J. G. Proakis, *Digital Communications*. New York: McGraw-Hill, 3rd ed., 1995.
- [8] J. Evans and D. Tse, "Large system performance of linear multiuser receivers in multipath fading channels," *IEEE Trans. Inf. Theory*, vol. 46, no. 6, pp. 2059–2078, 2000.
- [9] J. Benesty, Y. Huang, and J. Chen, "A fast recursive algorithm for optimum sequential signal detection in a BLAST system," *IEEE Trans. Signal Processing*, vol. 51, pp. 1722–1730, July 2003.
- [10] U. Fincke and M. Phost, "Improved methods for calculating vectors of short length in a lattice, including a complexity analysis," *Math. Comp.*, vol. 44, pp. 463–471, April 1985.
- [11] S. Verdú, *Multiuser Detection*. Cambridge (UK): Cambridge Univ. Press, 1998.